

Published in final edited form as:

*Cancer Res.* 2009 May 1; 69(9): 3731–3735. doi:10.1158/0008-5472.CAN-09-0096.

## Silibinin Feeding Alters the Metabolic Profile in TRAMP Prostatic Tumors: <sup>1</sup>H-NMRS-Based Metabolomics Study

Komal Raina<sup>1</sup>, Natalie J. Serkova<sup>2,3</sup>, and Rajesh Agarwal<sup>1,3,\*</sup>

<sup>1</sup>Department of Pharmaceutical Sciences, University of Colorado Denver, Aurora, Colorado

<sup>2</sup>Department of Anesthesiology and Radiology, University of Colorado Denver, Aurora, Colorado

<sup>3</sup>University of Colorado Cancer Center, University of Colorado Denver, Aurora, Colorado

### Abstract

Herein, we evaluated for the first time silibinin efficacy on prostate cancer (PCa) metabolism in transgenic adenocarcinoma of the mouse prostate (TRAMP) model utilizing quantitative high-resolution proton nuclear magnetic resonance spectroscopy (<sup>1</sup>H-NMRS) metabolomics. Prostate tissues were from mice fed control or silibinin diet for 20 weeks. Comparative metabolic profiling indicated that antitumor effect of silibinin is accompanied by alteration in metabolic profile of TRAMP prostatic tumors as indicated by 6 fold ( $P=0.016$ ) increase in glucose content and 48% ( $P=0.015$ ) reduction in lactate levels. Increase in citrate utilization by prostate tissue also reversed with silibinin, as indicated by 3-fold ( $P=0.01$ ) increase in citrate levels in silibinin-fed group. Also, 61% and 50% ( $P<0.01$ ) decrease in cholesterol and phosphatidylcholine levels, respectively, was observed with silibinin. These results corroborate our earlier findings regarding PCa chemopreventive potential of silibinin in TRAMP model and warrant additional metabolic profiling in other silibinin-fed PCa tumor model tissues. This will help identify specific metabolic biomarkers altered during silibinin treatment, which when detected in clinical biopsies or non-invasive MRS studies could help monitor silibinin effectiveness against PCa malignancy.

### Introduction

Recent studies have shown that metabolic profile of various cancerous/non-cancerous tissues can be correlated with cell growth/death, specific tumor type and pathological stage of tumor (1–4). In this regard, metabolomics of prostatic tissues using magnetic resonance spectroscopy (in both *in vivo* and *in vitro* conditions) has helped to identify and establish the metabolic profiles specific to prostate cancer (PCa) malignancy (1,5). Specific metabolic alterations, due to progression of tumor lesions in PCa patients, include a significant decrease of citrate (zinc metabolism), increased phosphocholine and phosphatidylcholine (phospholipid turnover), and increased glucose uptake in cancerous lesions (3,5).

We recently reported PCa inhibitory effects of silibinin in various studies (6) and on PCa progression in transgenic adenocarcinoma of the mouse prostate (TRAMP) mice (7). The chemopreventive efficacy of silibinin on TRAMP prostate tumor growth, progression, invasion, migration and metastasis was subsequently evaluated and established, together with analyses of the protein molecules possibly involved with silibinin efficacy (8). From a broader view point, the limitation of this study was that silibinin efficacy was not discussed in terms of metabolic stabilization in prostate tumors. With the rationale that evaluation of anticancer efficacy of a drug is incomplete without determining its effect on metabolic profile of the tumor

**Requests for reprints:** Rajesh Agarwal, email: E-mail: Rajesh.Agarwal@UCDenver.edu.

tissue, we carried out a metabolomics study on prostate tissues. We utilized quantitative high-resolution proton nuclear magnetic resonance spectroscopy ( $^1\text{H-NMRS}$ ) to assess the metabolic profile of silibinin-treated TRAMP prostatic tissue to complement histopathological and molecular data generated earlier (6–8). The working hypothesis was that, upon silibinin treatment, specific metabolic biomarkers will sensitively detect changes in prostate tissue. Such a study would, inarguably, not only provide us with a complete scenario of silibinin chemopreventive efficacy against PCa progression in TRAMP mice, but in terms of practical and translational aspects, further validate the clinical usefulness of this drug.

## Materials and Methods

### Prostate Tissue

Archival (7) dorsolateral prostate tissue (n=4) samples, stored at  $-80^\circ\text{C}$ , of TRAMP/C57BL/6 mice fed control (n=17) or 1% silibinin-supplemented diet starting 4-weeks of age for 20 weeks (n=16), were used to assess metabolic profile of tissues. All retrospective studies have been previously approved by our IACUC.

### Sample Preparation

Prostate tissues were extracted using 8% perchloric acid as previously described (4,9). Briefly, ~0.1 g of frozen tissues was processed, and extracted hydrophilic metabolites were dissolved in 0.45 mL of deuterium oxide ( $\text{D}_2\text{O}$ ) while lipids were dissolved in 0.6 mL of deuterated chloroform/methanol mixture (2:1, v/v) prior to  $^1\text{H-NMRS}$ . All deuterated compounds were from Cambridge Isotope Inc.

### Quantitative $^1\text{H-NMR}$ Analysis

$^1\text{H-NMRS}$  analyses were performed by NJS (blinded to the group assignment of samples) using a 500 MHz Bruker DRX system equipped with Bruker TopSpin software (Bruker Biospin Inc.) (9). An inverse TXI 5-mm probe was used for all experiments. To suppress water residue in extracts, a standard Bruker water presaturation sequence was used (“zgpr”). An external reference, trimethylsilyl propionic-2,2,3,3,-d<sub>4</sub> acid (TMSP, 0.5 mmol/L for hydrophilic and 1.2 mmol/L for lipid extracts), was used for metabolite quantification of fully relaxed  $^1\text{H-NMR}$  spectra and as a  $^1\text{H}$  chemical shift reference (0 ppm). For metabolite identification, a two-dimensional (2D)- $^1\text{H}$ ,  $^{13}\text{C}$ -HSQC (heteronuclear single quantum correlation) NMR sequence was used. The  $^1\text{H-NMR}$  peaks for single metabolites were identified and referred to a metabolite chemical shift library. The absolute concentrations of single metabolites were then referred to the TMSP integral and calculated using 1D WINNMR (Bruker Biospin Inc.) (9).

## Results

From each prostate tissue, 38 individual water-soluble and lipid metabolites were quantified (Table 1). We also included 4 significant metabolite ratios into the Principle component analysis (PCA), such that, for each tissue, a total set of 42 variables was included into the multivariate data analysis. The PCA analysis allowed for precise group separation between untreated and silibinin-fed TRAMP mice (Fig. 1A). In the next step, individual metabolites were distinguished, which were responsible for group clustering in Figure 1A. Total of 14 biomarkers contributed to group separation (Fig. 1B) and were related to citrate, glucose, phospholipid, osmolyte and antioxidant metabolism (Fig. 2). The major contributors for group separations were increased concentrations for citrate, intracellular glucose, choline in the water-soluble fraction, glycerophosphocholine (GPC) and myo-inositol, as well as decreased values of lactate, cholesterol and three ratios from glucose and phospholipid metabolism. To lesser extent, decreased alanine and phosphatidylcholine, but increased polyols, glutathione and the ratio of unsaturated fatty acids contributed to the group clustering.

One of the most important findings in this study is the preserved citrate concentration in prostate upon silibinin treatment, as indicated by ~3 fold ( $p < 0.01$ ) increase in citrate levels in silibinin group (Fig. 2A). That the citrate generated for normal secretion functions of the prostate and zinc metabolism was not further utilized for cholesterol synthesis was indicated by 61% decrease ( $p < 0.04$ ) in cholesterol levels in silibinin-fed group, indicating decreased cholesterogenesis (Fig. 2C).

Further, a significant decrease in glucose utilization was seen in silibinin-fed animals. Increased glucose uptake, due to high energy requirement and high aerobic glycolytic activity – one of the major hallmarks of tumor metabolism – usually results in decreased intracellular glucose concentrations and high levels of lactate (10,11). In our study, a significant increase in intracellular glucose ( $p < 0.01$ ) with simultaneous decrease in lactate ( $p < 0.01$ ) and alanine ( $p < 0.03$ ) (end-products of glycolysis) were seen after silibinin-feeding (Fig. 2A). Thus, the glycolytic coefficient (ratio of intracellular lactate to intracellular glucose) was decreased from 26.68 in controls to 2.66 in silibinin-fed animals ( $p < 0.05$ , Table 1, Fig. 2A).

Another significant metabolic pathway for tumor development is increased phospholipid turnover in cancer cells, due to their high proliferation rates (12). In a variety of tumors, phosphatidylcholine (PtdCho), the major phospholipid in cell membrane, is increased (13, 14). Silibinin not only decreased PtdCho values in prostate ( $p < 0.03$ , Fig. 2B), but also significantly altered PtdCho synthesis and catabolism, thus providing an evidence for targeted cell growth inhibition. The ratio of phosphocholine (PC - PtdCho precursor) to glycerophosphocholine (GPC - PtdCho catabolism) was significantly decreased after silibinin treatment ( $p < 0.04$ ), mostly due to an increase in GPC concentrations ( $p < 0.01$ ). Moreover, a significant inhibition of PtdCho synthesis can be seen in accumulation of cytosolic hydrophilic choline ( $p < 0.01$ ) and its dramatically decreased incorporation into membrane lipid fraction: the ratio of lipid-derived choline to cytosolic choline decreased from 67.6 to 4.1 in silibinin-fed animals ( $p < 0.0001$ , Table 1, Fig. 2B).

Increased concentrations of osmolyte myo-inositol ( $p < 0.0001$ ) and other polyols ( $p < 0.03$ ) were also observed in silibinin-fed group (Fig. 2C). Normal prostate glands express relatively high concentrations of polyols compared to PCa lesions. Higher levels of glutathione ( $p < 0.04$ ) and decreased [PUFA/MUFA] ratios ( $p < 0.05$ ) indicated improved anti-oxidant defense and decreased necrotic fraction under silibinin treatment.

## Discussion

PCa progression in TRAMP mice mimics human PCa; developing spontaneous progressive stages of the prostatic disease with time (15–17). Earlier studies in TRAMP model indicate that silibinin reduces prostate adenocarcinoma incidence by slowing down tumor progression from prostatic intraepithelial neoplasia (pre-malignant) to adenocarcinoma (malignant) stages (7).

In the present study, metabolic profiling of TRAMP prostate tissues appeared to be highly sensitive to oral silibinin supplementation. Silibinin-related metabolic changes include: (i) normalization of citrate concentrations (for normal secretory functions of prostate); (ii) decrease of glucose utilization and glycolytic activity; (iii) decrease in membrane phospholipid synthesis; and (iv) increase in polyols and antioxidants in prostate.

The results indicate that there is decreased glucose utilization by the prostatic tissue upon silibinin-feeding which suggests decreased bioenergy requirements via fast glycolysis compared to untreated tumors which are highly proliferative and consume more glucose to meet their increased energy requirements. Thus, due to high activity of aerobic glycolysis in the untreated tumors, an increase in the end products of glycolysis (lactate and alanine) can be

seen. There was also a significant reduction in lactate and alanine levels in silibinin-treated prostatic tissue which resulted in decreased glycolytic coefficient.

Alteration in citrate levels upon PCa progression in TRAMP mice was found to mimic human PCa scenario, where a decrease in citrate levels is observed due to its increased utilization in Krebs cycle as well as to abnormal secretion functions and zinc metabolism. In normal human prostate, the glandular epithelial cells follow a metabolic pathway unlike other normal tissues (11,18). In normal prostate epithelial cells (PEC), citrate is not an utilizable intermediate in Krebs cycle, but an end product. This is likely due to accumulation of high levels of zinc in PEC of peripheral zone (the zone involved in PCa malignancy) than in other normal tissues (19). Zinc is involved in inhibition of m-aconitase (which converts citrate into iso-citrate in Krebs cycle), which results in an increase in net citrate production; the high amount of citrate is then secreted in the prostatic fluid. Thus normal PEC unlike other normal mammalian cells are citrate producing cells (18). Unlike other tumor types which end up being citrate producing, the malignant PEC have decreased levels of citrate as a consequence of decreased amounts of zinc (18). As a result, m-aconitase activity is not inhibited and citrate is utilized by the Krebs cycle. While in normal PEC, 60% of energy derived from glucose is wasted due to citrate secretion, in malignant PEC, utilization of citrate in the Krebs cycle causes increased energy production and fatty acid synthesis in order to fulfill energy requirement of the fast proliferating PEC (18). These altered metabolic phenotype explains morphological transformation from normal secretion cells to the fast proliferative tumor cells and is an essential metabolic adaptation to meet the increased bioenergetic demands of the neoplastic cells (11,20). In the present study, one of the most significant observations was that silibinin was able to cause a reversal of citrate utilization in tumor cells and helped preserve the citrate concentration in prostatic tissue as it occurs in normal prostatic tissue i.e., silibinin was able to restore the citrate producing characteristic and secretion functions of the prostatic tissue. Further, decrease in cholesterologenesis indicated that increased citrate was not being utilized for this process.

A variety of cancerous tissues including that of prostate exhibit altered metabolic profile of choline pathway intermediates (12,13), specifically, the malignant tissues are characterized by elevated levels of Ptd-Cho, the major membrane phospholipid, along with high levels of its precursor, PC (13,14). Silibinin significantly decreased Ptd-Cho levels and altered the Ptd-Cho turnover in prostatic tissue as evidenced by increased GPC levels (Ptd-Cho catabolic product) and a decrease in the content of lipid derived choline. The decreased ratio of PC/GPC by silibinin was also an interesting observation, as in some cancer cells a switch from high GPC levels and low PC levels to low GPC and high levels of PC has been observed with increased malignancy (13). Whether this decrease in ratio by silibinin in TRAMP prostate can be interpreted as a positive inhibitory effect specific to TRAMP or is a general interference in choline phospholipid metabolism by silibinin, needs to be further investigated.

Silibinin feeding also significantly increased polyol levels which are significantly decreased during prostate tumor progression. There was also a significant increase in total glutathione levels in prostatic tissue by silibinin-feeding compared to untreated controls, indicating that silibinin plays an inhibitory role in the progression of PCa by increasing the levels of the antioxidant glutathione, which serves as a free radical scavenger.

Whether the inhibitory effects of silibinin on PCa progression in TRAMP mice are via a direct interference in the metabolic pathway of various metabolites associated with malignancy in this PCa model or are a consequence of the normalizing effect that silibinin has on the malignant tissue via a genomic/proteomic response needs to be further investigated.

To the best of our knowledge, this is the first study of its kind, where the chemopreventive efficacy of an agent has also been evaluated in terms of the metabolomics of the tumors. The

results corroborate our earlier findings and indicate the essential need to carry out such metabolic profiling in various other PCa tumor model tissues following treatment with a chemopreventive agent, including silibinin, so as to help identify the specific metabolites altered during the course of treatment, which when detected in clinical biopsies or non-invasive MRS studies can confirm the effectiveness of the agent against PCa malignancy.

## Acknowledgements

We thank Andrea Merz, B.S., for sample extraction. Metabolomics NMR Cancer Center Core facility was partly supported by Anesthesiology Department and NCI P30 CA046934 Cancer Center Core Grant.

**Grant support:** NCI RO1 CA102514 and P30 CA046934.

## References

1. Griffin JL, Kauppinen RA. Tumour metabolomics in animal models of human cancer. *J Proteome Res* 2007;6:498–505. [PubMed: 17269706]
2. Griffin JL, Shockcor JP. Metabolic profiles of cancer cells. *Nat Rev Cancer* 2004;4:551–561. [PubMed: 15229480]
3. Serkova NJ, Spratlin JL, Eckhardt SG. NMR-based metabolomics: translational application and treatment of cancer. *Curr Opin Mol Ther* 2007;9:572–585. [PubMed: 18041668]
4. Serkova NJ, Niemann CU. Pattern recognition and biomarker validation using quantitative <sup>1</sup>H-NMR-based metabolomics. *Expert Rev Mol Diagn* 2006;6:717–731. [PubMed: 17009906]
5. Serkova NJ, Gamito EJ, Jones RH, et al. The metabolites citrate, myo-inositol, and spermine are potential age-independent markers of prostate cancer in human expressed prostatic secretions. *Prostate* 2008;68:620–628. [PubMed: 18213632]
6. Singh RP, Agarwal R. Prostate cancer prevention by silibinin – bench to bedside. *Mol Carcinogenesis* 2006;45:436–442.
7. Raina K, Blouin MJ, Singh RP, et al. Dietary feeding of silibinin inhibits prostate tumor growth and progression in transgenic adenocarcinoma of the mouse prostate model. *Cancer Res* 2007;67:11083–11091. [PubMed: 18006855]
8. Raina K, Rajamanickam S, Singh RP, et al. Stage-specific inhibitory effects and associated mechanisms of silibinin on tumor progression and metastasis in transgenic adenocarcinoma of the mouse prostate model. *Cancer Res* 2008;68:6822–6830. [PubMed: 18701508]
9. Serkova NJ, Rose JC, Epperson LE, Carey HV, Martin SL. Quantitative analysis of liver metabolites in three stages of the circannual hibernation cycle in 13-lined ground squirrels by NMR. *Physiol Genomics* 2007;31:15–24. [PubMed: 17536023]
10. Baggetto LG. Deviant energetic metabolism of glycolytic cancer cells. *Biochimie* 1992;74:959–974. [PubMed: 1477140]
11. Costello LC, Franklin RB. 'Why do tumour cells glycolyse?': from glycolysis through citrate to lipogenesis. *Mol Cell Biochem* 2005;280:1–8. [PubMed: 16511951]
12. Ackerstaff E, Glunde K, Bhujwalla ZM. Choline phospholipid metabolism: a target in cancer cells? *J Cell Biochem* 2003;90:525–533. [PubMed: 14523987]
13. Glunde K, Serkova NJ. Therapeutic targets and biomarkers identified in cancer choline phospholipid metabolism. *Pharmacogenomics* 2006;7:1109–1123. [PubMed: 17054420]
14. Glunde K, Jacobs MA, Bhujwalla ZM. Choline metabolism in cancer: implications for diagnosis and therapy. *Expert Rev Mol Diagn* 2006;6:821–829. [PubMed: 17140369]
15. Gingrich JR, Barrios RJ, Foster BA, Greenberg NM. Pathologic progression of autochthonous prostate cancer in the TRAMP model. *Prostate Cancer Prostatic Dis* 1999;2:70–75. [PubMed: 12496841]
16. Greenberg NM, DeMayo FJ, Sheppard PC, et al. The rat probasin gene promoter directs hormonally and developmentally regulated expression of a heterologous gene specifically to the prostate in transgenic mice. *Mol Endocrinol* 1994;8:230–239. [PubMed: 8170479]
17. Gingrich JR, Greenberg NM. A transgenic mouse prostate cancer model. *Toxicol Pathol* 1996;24:502–504. [PubMed: 8864193]

18. Costello LC, Franklin RB. The intermediary metabolism of the prostate: a key to understanding the pathogenesis and progression of prostate malignancy. *Oncology* 2000;59:269–282. [PubMed: 11096338]
19. Costello LC, Franklin RB. The clinical relevance of the metabolism of prostate cancer; zinc and tumor suppression: connecting the dots. *Mol Cancer* 2006;5:17. [PubMed: 16700911]
20. Costello LC, Franklin RB. Tumor cell metabolism: the marriage of molecular genetics and proteomics with cellular intermediary metabolism; proceed with caution! *Mol Cancer* 2006;5:59. [PubMed: 17090311]



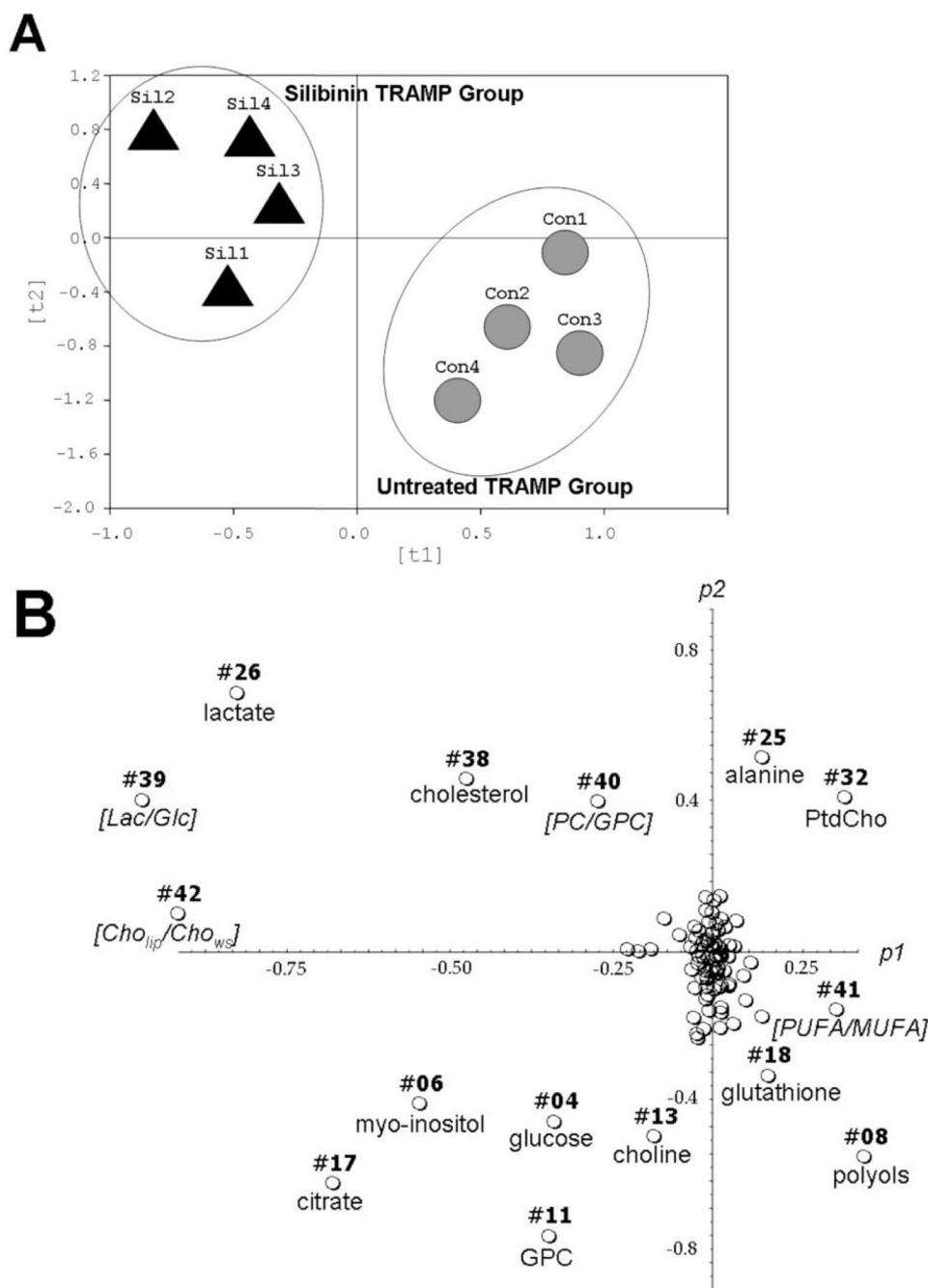


**Fig. 1.** Principle component analysis (PCA) on quantitative data sets for water-soluble and lipid metabolites, calculated from  $^1\text{H-NMR}$  spectra of prostate tissue extracts. (A) PCA scores ( $t_i$ ) based on global metabolic pattern showed group separations between control and silibinin-treated TRAMP mice. (B) PCA plots ( $p_i$ ) on absolute concentrations of individual metabolites distinguish single putative biomarkers responsible for clustering pattern observed in panel A. Each circle represents an individual metabolite, which is assigned as a number of metabolite, according to Table 1. Briefly, PCA was applied to quantitative sets, which consisted of absolute individual concentrations of all metabolites obtained from two  $^1\text{H-NMRS}$  data sets for each sample ( $^1\text{H-NMR}$  on water-soluble and lipid fractions). PCA prediction/ classification (group

clustering or “pattern recognition” visualization) and all mathematical models were built with AMIX software (3.5.1., Bruker Biospin Inc) followed by R package (2.00) on absolute concentrations of water-soluble and lipophilic metabolites.



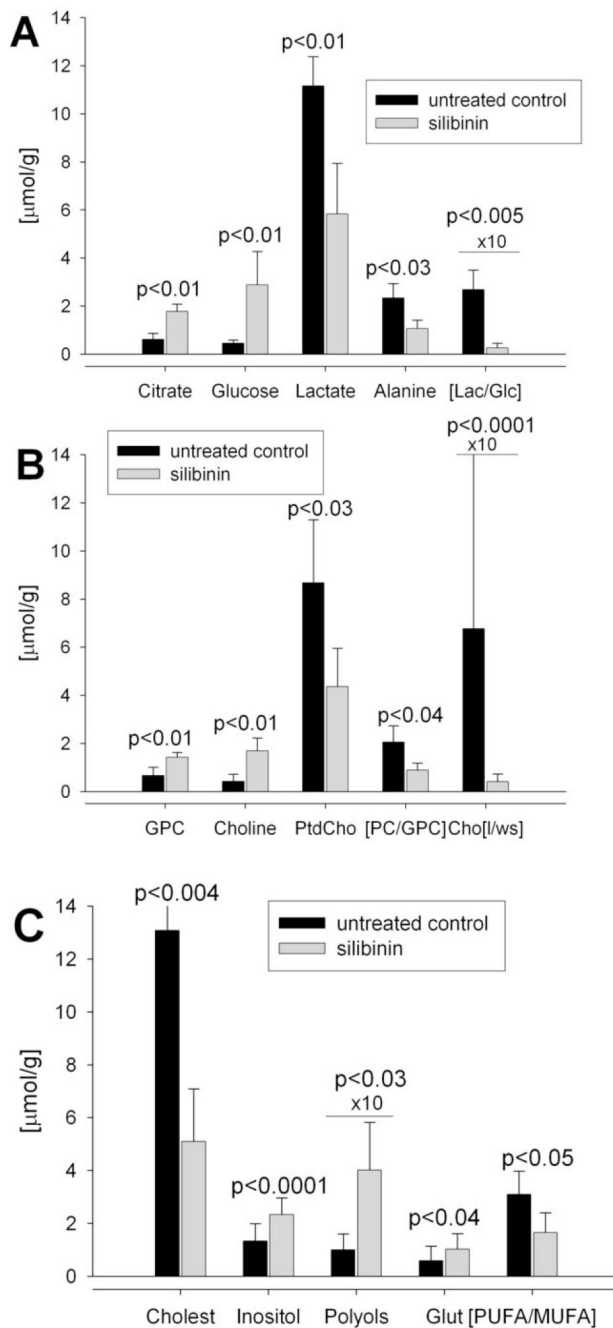


**Fig. 2.** Validation of metabolites that were distinguished as biomarkers for metabolic changes following silibinin treatment (see Figure 1B). Panels A–C plot individual concentrations ( $\mu\text{mol/g}$ ) prostate tissue,  $n=4$  for each data set) for each metabolite or metabolite ratios as calculated from  $^1\text{H-NMR}$  spectra of hydrophilic and lipophilic fractions (Table 1).

**Table 1**  
Quantitative metabolic profile of prostatic tumor tissues of two study groups: (i) control untreated TRAMP mice, and (ii) silibinin-treated TRAMP mice (1% w/w silibinin supplemented diet given for 20 weeks).\*

Metabolite	<sup>1</sup> H-NMRS	δ, ppm	Untreated [μmol/g]	Silibinin [μmol/g]
1. Aromatic Amino Acids	hydrophilic	9.28-6.85	8.19±3.77	12.71±7.14
2. Adenine	hydrophilic	6.00	0.65±0.75	0.24±0.11
3. Adenosine	hydrophilic	5.87	0.47±0.42	0.59±0.49
4. Glucose	hydrophilic	5.23+4.64	0.45±0.14	2.88±1.39 p<0.01
5. Nucleotides	hydrophilic	4.43	0.93±1.16	1.01±0.94
6. Myo-Inositol	hydrophilic	4.05	1.34±0.65	2.34±0.62 p<0.0001
7. Creatine	hydrophilic	3.93	2.04±1.95	2.58±0.63
8. Polyols	hydrophilic	3.82-3.58	10.04±5.92	40.16±18.05 p<0.03
9. Glycine	hydrophilic	3.56	2.53±0.79	2.96±1.23
10. Taurine	hydrophilic	3.43+3.26	9.38±4.34	10.75±0.70
11. GPC	hydrophilic	3.23	0.67±0.34	1.43±0.20 p<0.01
12. PC	hydrophilic	3.21	1.44±1.24	2.19±1.56
13. Total Choline	hydrophilic	3.19	0.43±0.29	1.70±0.53 p<0.01
14. Total Creatine	hydrophilic	3.03	2.64±1.63	5.29±1.30
15. GSH	hydrophilic	2.95	0.36±0.55	0.67±0.27
16. Aspartate	hydrophilic	2.82+2.63	0.33±0.16	0.29±0.05
17. Citrate	hydrophilic	2.66+2.53	0.61±0.26	1.78±0.30 p<0.01
18. Total Glutathione	hydrophilic	2.48	0.59±0.54	1.03±0.59 p<0.04
19. Glutamine	hydrophilic	2.43	0.47±0.29	0.47±0.21
20. Succinate	hydrophilic	2.40	0.94±0.20	0.98±0.19
21. Glutamate	hydrophilic	2.35	2.54±1.45	3.07±0.26
22. Total CH <sub>2</sub> -CH <sub>3</sub>	hydrophilic	2.25-1.95	4.37±2.72	6.55±0.89
23. Acetate	hydrophilic	1.91	0.79±0.37	0.85±0.54
24. Arginine+Lysine	hydrophilic	1.73-1.67	0.80±0.49	0.99±0.10
25. Alanine	hydrophilic	1.47	2.33±0.61	1.07±0.34 p<0.03
26. Lactate	hydrophilic	1.32	11.16±1.21	5.83±2.11 p<0.01
27. Hydroxybutyrate	hydrophilic	1.19	0.29±0.12	0.60±0.29
28. Essential Amino Acids	hydrophilic	1.10-0.72	4.97±2.87	5.88±1.41

Metabolite	<sup>1</sup> H-NMRS	δ, ppm	Untreated [μmol/g]	Silibinin [μmol/g]
29. MUFA	lipids	5.42	20.48±6.33	43.61±29.05
30. Triacylglycerol	lipids	4.18	9.52±2.72	21.47±16.96
31. Glycerol-Lipids	lipids	4.13–4.07	2.89±2.11	5.89±2.64
32. PtdCho	lipids	3.65	8.68±2.61	4.36±1.59 <sup>p&lt;0.03</sup>
33. Total Cholines (Lipids)	lipids	3.22	13.31±6.46	5.88±2.78
34. PtdEth	lipids	3.19	1.94±1.41	1.24±0.73
35. PUFA	lipids	2.82	60.02±9.13	48.68±14.51
36. Total Fatty Acids	lipids	2.28	78.57±17.55	114.74±60.50
37. Total Lipids	lipids	0.89	142.29±30.92	163.93±73.52
38. Cholesterol	lipids	0.68	13.07±1.48	5.09±2.00 <sup>p&lt;0.004</sup>
39. [Lactate/ Glucose]	hydrophilic	n/a	26.68±8.20	2.66±1.93 <sup>p&lt;0.005</sup>
40. [PC/ GPC]	hydrophilic	n/a	2.05±0.68	0.89±0.30 <sup>p&lt;0.04</sup>
41. [PUFA/MUFA]	lipids	n/a	3.09±0.88	1.66±0.74 <sup>p&lt;0.05</sup>
42. [Cho <sub>lipids</sub> / Cho <sub>hydrophilic</sub> ]	n/a	n/a	67.57±78.33	4.05±3.19 <sup>p&lt;0.0001</sup>

\* All data are given in μmol per g prostate tissue and presented as mean ±S.D. (n=4 for each group). Absolute individual concentrations of distinguished biomarkers were analyzed by ANOVA followed by Tukey's post-hoc test to identify the groups that differed significantly. The significance level was set at p<0.05 for all tests (Sigma Plot-version 9.01, Systat Software and SPSS version 14.0, SPSS Inc). Only selected <sup>1</sup>H-chemical shifts are reported for individual metabolites (which were used for metabolite quantification). Cho [l/wt], ratio of cholines in lipid and water-soluble fractions. Cho, choline; GPC, glycerophosphocholine; GSH, reduced glutathione; MUFA, mono-unsaturated fatty acids; PC, phosphocholine; ppm, part per million (units for NMR chemical shifts); PtdCho, phosphatidylcholine; PtdEth, phosphatidylethanolamine; PUFA, poly-unsaturated fatty acids.